Swiss Journal of Geosciences (2019) 112:435–451
https://doi.org/10.1007/s00015-019-00343-4

Examination of a relationship between atmospheric blocking and seismic events in the Middle East using a new seismo-climatic index

Mohammad Reza Mansouri Daneshvar[1] · Friedemann T. Freund[2]

Received: 8 May 2019 / Accepted: 1 August 2019 / Published online: 14 August 2019

Abstract
This study statistically examines the role of atmospheric blocking as a precursor of major seismic events. Atmospheric blocking archive and earthquake databases for the Middle East region are compiled for 2000–2013. Correlations between atmospheric blocking events and seismicity are examined based on defined seismo-climatic index (SCI) based on variations of earthquake frequency and magnitude before and after blocking events. Limiting the SCI index to values > 6, 16 out of 26 major earthquakes ($M > 6$), i.e. 62%, are shown to have occurred within 14 days after blocking events over their respective epicentral regions. The correlation between blocking events and subsequent seismicity falls into a range of 0.694–0.803. Additional blocking-related atmospheric anomalies such as cyclogenesis, cloud coverage, and anomalous rainfall prior to major earthquakes can be understood as processes that take place in the Earth's crust and at the ground-to-air interface as a result of the stress activation of positive hole charge carriers at depth, in the hypocentral rock volume, and their rapid migration to the Earth's surface. Hence, atmospheric blocking events in a seismically active region may be categorized as an earthquake precursory phenomenon.

Keywords Atmospheric blocking · Seismo-climatic index · Seismicity · Earthquake frequency and magnitude · Middle East

1 Introduction

The term "atmospheric blocking" describes patterns that involve local or regional high-pressure or low-pressure systems on the scale of hundreds of kilometers, which can be quasi-stationary, persisting for days, even weeks (Pelly and Hoskins 2003). This phenomenon raises the question: Are there identifiable causes other than fortuitous patterns of stagnant air masses, which can lead to blocking? Scherrer et al. (2006) pointed to several reasons such as a bifurcation of zonal flows leading to modons (McWilliams 1980; Verkley 1990), planetary wave interaction (Hansen and Sutera 1984; Lindzen 1986; Lejenäs and Döös 1987) possible interaction between orographic forcing and non-linear wave flows (Egger 1978; Da Silva and Lindzen 1993), multiple equilibria and resonances (Charney and Devore 1979) or an interaction between synoptic and planetary-scale processes (Shutts 1983; Lupo and Smith 1995). All these processes are distinctly atmospheric in nature in as much as that they do not consider any specific interactions with the Earth's surface, either water or land, except for interactions driven by insolation and its effect on the thermal input into the atmosphere.

However, there are known physical processes taking place inside the Earth's crust, which can lead to pronounced interactions with the atmosphere. These processes are linked to tectonic stresses waxing and waning inside the Earth's crust. These stresses express themselves through a range of observable pre-earthquake phenomena such as

Editorial Handling: S. Schmid.

✉ Mohammad Reza Mansouri Daneshvar
mrm_daneshvar2012@yahoo.com
http://www.researcherid.com/rid/G-2881-2012

Friedemann T. Freund
friedemann.t.freund@nasa.gov

[1] Department of Geography and Natural Hazards, Research Institute of Shakhes Pajouh, Isfahan, Iran

[2] GeoCosmo Science and Research Center, NASA Ames Research Park, Code SCR, M, Moffett Field, CA 94035-1000, USA

electric currents flowing in the crust, anomalous infrared emissions in the thermal band off the Earth's surface in regions subjected to tectonic stressing, generation of massive amounts of positive and negative airborne ions at the Earth's surface, which most likely are a part of the global electrical circuit (Freund 2013). There are also many reports about the prevalence of cloud formation, thunderstorm, and cyclogenesis prior to major earthquakes (Dubrov et al. 2014). Here we look in greater detail at these interactions between the Earth's crust, the Earth's surface and atmospheric processes, specifically extreme events such as blocking.

The essence of block formation describes a high pressure (anticyclone) with low-potential vorticity, which extends pole-ward over a large-amplitude slow-moving cyclone (Pelly and Hoskins 2003). Atmospheric blocking and its quasi-stationary nature can maintain thunderstorms, cyclogenesis, and abnormal values of atmospheric vorticity. In this study, the locations of quasi-stationary cyclones, which have been observed over the study regions, were considered to next statements, not the locations of anticyclones. Consistent with this approach, some researchers have examined the intensity of upstream cyclogenesis, which is dynamically associated with blocking events (e.g., Konrad and Colucci 1988; Tsou and Smith 1990; Lupo and Smith 1995; Lupo 1997). The abnormal characteristics mentioned here have direct synergic effects on the formation of cyclones through the dipole type patterns of split flow and cutoff blockings. These blocking types can set in after atmospheric disturbances (McWilliams 1980; Verkley 1990).

Lithosphere-atmosphere interactions in the context of pre-earthquake conditions have been discussed extensively assuming that the emanation of radioactive radon from the Earth's surface is the main driver for increased air ionization, leading to perturbations in the atmosphere (Pulinets et al. 1997; Ondoh 2003; Dunajecka and Pulinets 2005; Pulinets 2006; Ouzounov et al. 2007; Pulinets and Ouzounov 2010; Pulinets et al. 2010; Pulinets 2011; Klimenko et al. 2011; Pulinets and Ouzounov 2011; Pulinets et al. 2014).

The emanation of radon from the ground and its release into the groundwater or spring waters indeed change as a function of time prior to local and regional seismic activity, typically by a factor between 2 and 20 (Inan et al. 2010). For instance, the volumetric activity of radon before a local earthquake in Lebanon has been reported as an extreme value with over than 2500 kBq/m^3 by Kobeissi et al. (2015). Moreover, Dunajecka and Pulinets (2005), Pulinets et al. (2006), Pulinets and Dunajecka (2007), and Ouzounov et al. (2011) reported meteorological variations induced by radon emanation and air ionization during the preparational stage of many earthquakes. Radon is an extreme trace gas that can be measured by counting the radioactive decay events of individual atoms. However, the radon content in the entire Earth's atmosphere is only a few tens of grams, continuously replaced by the decay of radium and uranium and released from the ground.

This study attempts to describe a very different process, by which air ions are episodically injected into the atmosphere at the Earth's surface, namely a process that is driven by the build-up of tectonic stresses in the Earth's crust prior to the seismic activity. This process involves the activation of highly mobile electronic charge carriers in the rock column when mechanical stresses act on the matrix of rocks, shifting mineral grains relative to each other that contain peroxy defects along or across their grain boundaries, typically $O_3Si–OO–SiO_3$.

Peroxy defects exist in all igneous and high-grade metamorphic rocks as well as in sedimentary rocks containing detrital mineral grains from igneous rocks (Freund and Freund 2015). Many peroxy defects reside on or straddle across grain boundaries, making them susceptible to being activated by mechanical deformation of the rocks, which causes grain movements relative to each other (Scoville et al. 2015). The activation proceeds through an electron transfer from a neighboring O^{2-}, which thereby turns into O^-, i.e., a defect electron in the oxygen anion sublattice, known as a positive hole. Positive holes have the remarkable ability to flow out of the stressed rock volume, propagating fast (at speeds up to about 100 m/s) and far (over distances on the order of tens of kilometers and more[1]). As the positive holes arrive at the Earth's surface, they accumulate in a thin subsurface charge layer (King

[1] There are only indirect data available about the distances over which positive holes can travel through the Earth's crust or about the losses they incur. If we accept that telluric currents, ground potentials, surface ionization and a host of other pre-earthquake phenomena are all caused by positive hole charge carriers, it is clear that the distances over which positive holes can travel are on the order of tens of kilometer. Example #1: From the strength of the magnetic field fluctuations (max 30 nT) measured prior to the M = 5.6 Alum Rock earthquake of Oct 30, 2007, in California, the telluric currents presumed to flow at the hypocenter depth of ~ 10 km were calculated to be in the 10^4–10^5 amp range (Bortnik et al. 2010). At the same time, massive air ionization occurred at the surface, implying that the same positive hole charge carriers, which produce the telluric currents at depth, had traveled from 10 km depth to the Earth surface. Example #2: In the case of the M = 7.6 Chi-Chi earthquake of Sep 21, 1999, in Taiwan, the magnetic field fluctuations up to 250 nT for an event with a hypocenter depth of ~ 20 km, suggesting currents on the order of 10^6 amps (Freund and Pilorz 2012). These telluric currents were flowing laterally across about ½ of the island of Taiwan, which measures ~ 500 km in the North–South direction. Example #3: We could also reference a paper on the animal response in the Peruvian Andes, where an M = 7 earthquake occurred at a depth of 140 km about 370 km lateral distance from our observation site (Grant et al. 2015). If the animal behavior was triggered by positive holes stress-activated in the hypocentral volume, the charge carriers must have traveled these distances.

and Freund 1984). The associated electric field readily reaches values high enough to initiate field ionization of air molecules, preferentially O_2, which has the lowest ionization potential (Freund et al. 2009).

Geologically the silicate matrix of basement rocks is generated below the bulk of the lithosphere (Crepisson et al. 2014) and is gravitationally altered between continental and oceanic crust. Hence, the effect of positive-hole charge carriers could be noticeable across the entire Earth's crust because it is linked to the silicate matrix of basement rocks, irrespective of continental or oceanic characteristics. Published evidence (Freund 2013; Freund and Freund 2015; Scoville et al. 2015) strongly suggested that all rocks could contain peroxy defects irrespective of their petrological origin, be it continental or oceanic crust, or high-grade metamorphic material. Even regular sedimentary rocks that contain detrital grains of, for instance, quartz or feldspars from crystalline rocks carry peroxy and do respond accordingly to mechanical stresses.

As shown in Fig. 1a and b air ionization events have occurred before major seismic activity, in this case the M = 5.6 Alum Rock earthquake of Oct. 30, 2003, in northern California, USA (Bleier et al. 2009), and at many other locations such as in Japan (Yada and Saito 2012). These ionization events can lead to large changes in the air ion concentrations by a factor of more than 1000. When recorded close to the epicenter as was the case prior to the 2003 Alum Rock earthquake, local variations in the air ionization can occur very rapidly, within tens of seconds, producing repetitive pulses that last only minutes as strikingly demonstrated in Fig. 1b.

The speed with which these air ionization pulses occur, their quasi-periodicity, their large areal extent up to 100 km across (Yada and Saito 2012), and their rapid intensity variations make them prime candidates to produce atmospheric anomalies (Mansouri Daneshvar et al. 2014b). Air ions act as nuclei for water vapor condensation, which in turn leads to increased latent heat flux in the atmosphere (Svensmark et al. 2007). Thus, air laden with ions due to pre-earthquake activities can cause meteorological effects by contributing to cloud formation and rainfall through the condensation of moisture, increased latent heat release, strong thermal updrafts and build-up of thunderstorms (D'Alessandro 2009; Tammet et al. 2009; Kolarž et al. 2012; Santos et al. 2015).

Pfahl et al. (2015) indicate that the diabatic ascent of air from lower altitudes due to latent heating in clouds is of first-order importance for the formation and maintenance of blocking. Such diabatic ascents of air masses could be related to the release of heat, directly or indirectly, from the tectonically active lithosphere. Furthermore, Mansouri Daneshvar et al. (2015) proposed a new concept, distinctly interdisciplinary, based on atmosphere-lithosphere interactions that relate the triggering of atmospheric blocking to lithospheric gas emanations, rainfall-induced stresses, and cyclogenesis before major seismic activity. As an example, a series of dipole type blocking events across southern Iran in April 2013 seems to have been related to pre-earthquake atmospheric anomalies linked to the M 6.4 Bushehr, M 7.8 Saravan and M 6.1 Angohran events. Mansouri Daneshvar and Freund (2017) argued that atmospheric and ionospheric anomalies, changes in cloud coverage and daily precipitation, changes in the sea-level air pressure and the geopotential height at 1000 and 500 hPa, in the daily stream function and v-wind and u-wind vectors, as well as trace gases such as O_3 and SO_2, and an abnormal cyclone over the epicentral region prior the M 8.3 Illapel earthquake of September 16, 2015 are consistent with air ionization

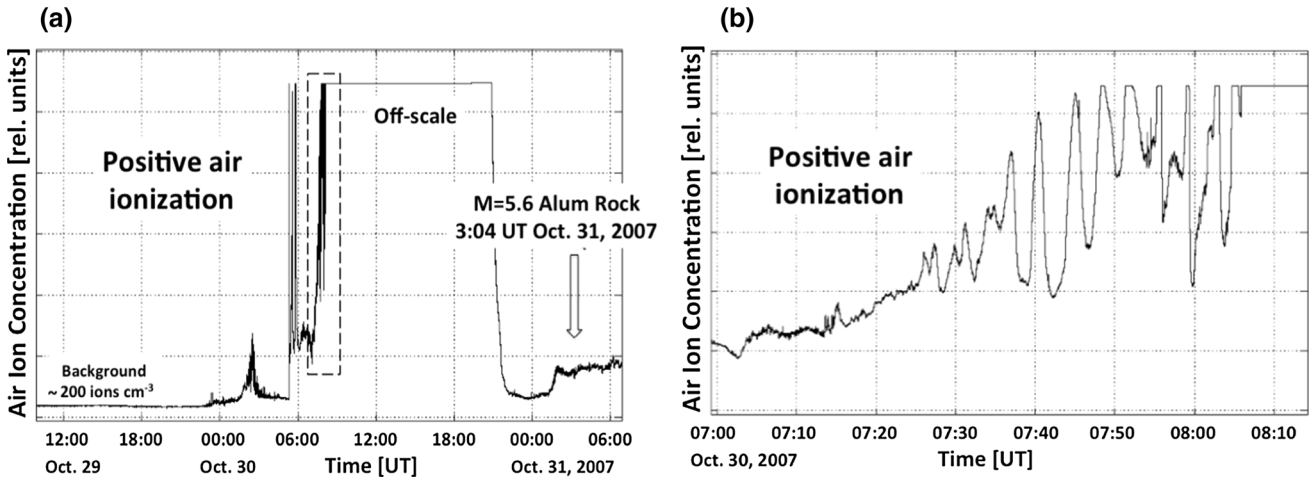

Fig. 1 **a** Positive air ionization prior to the M = 5.6 Alum Rock earthquake in Northern California starting ~ 24 h before the seismic event with a 12 h long off-scale section, reaching an estimated concentration of positive air ions of 10^5 cm^{-3}, recorded < 2 km from the epicenter. **b** Enlarged section showing rapid, repetitive changes in air ion concentrations (Bleier et al. 2009)

processes at the ground-to-air interface arising from the stress activation of peroxy defects within the hypocentral volume.

The present study examines how atmospheric blocking events can be used to derive information about impending seismic activity. By using a new statistical approach, this study is based on the analysis of the seismic activity in the broad region of the Middle East from 2000 to 2013.

2 Atmospheric blocking research

The term "atmospheric blocking" is used to describe a perturbation of tropospheric Rossby waves at mid-latitudes, associated with a split in the zonal jet and ridging at higher latitudes (Rex 1950; Illari 1984). The formation of an atmospheric block by Rossby wave breaking is depicted in Fig. 2. Berrisford et al. (2007) have argued that the Rossby wave breaking entails removal or reversal of the usual meridional gradients and shears, replacing them with blocks. However, Hitchman and Huesmann (2007) counterargued that, in much of the troposphere, wave breaking should not be expected to result in blocking.

Huang et al. (2007) pointed out that atmospheric blocking usually involves three types of interactions: monopole (Ω-type blocking), dipole (McWilliams 1980; Malguzzi and Malanotte-Rizzoli 1984) and multi-pole (Luo 2005). The formation of blocking events in the northern hemisphere has been studied widely. Their basic pattern is of the dipole type and always occurs during weak westerlies (Shutts 1983; Luo et al. 2001; Luo 2005). According to de Vries et al. (2013), stationarity and persistence of blocking, combined with anomalous-flow conditions, account from many cases of extreme weather (Trigo et al. 2004; Sillmann and Croci-Maspoli 2009; Cattiaux et al. 2010; Sillmann et al. 2011; Buehler et al. 2011; de Vries et al. 2012).

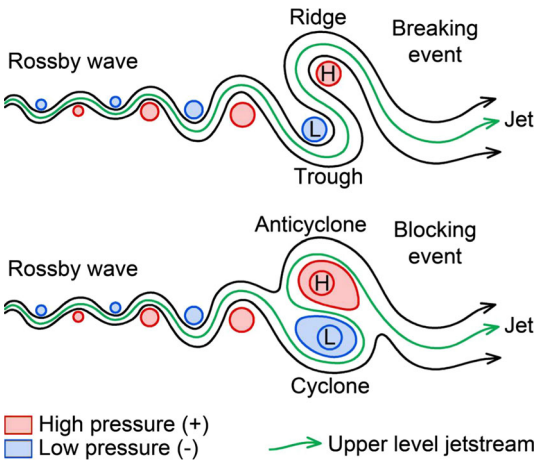

Fig. 2 Schematic 2-D projection of Rossby wave, upper level jet stream, and breaking way to produce an atmospheric blocking event

As a dynamic process in the atmosphere, blocking plays an important role in the mid-latitude climate variability and the anomalous climatic means and extremes (Sillmann and Croci-Maspoli 2009). Pelly and Hoskins (2003) propose that the concept of atmospheric blocking may be extended to define blocking episodes, which take into account the persistence of blocking along with a given longitude in a day. This definition provided an explanation why the blocking features, identified daily, are able to move longitudinally, with the onset of a blocking event being defined as the first day of a 4-day period of blocked air flow (Pelly and Hoskins 2003).

According to Scherrer et al. (2006), Doblas-Reyes et al. (2002) divided blocking detection methods into objective and subjective groups. Objective detection uses statistical methods to classify the circulation patterns (Vautard 1990). However, most common blocking indicators are subjective in the sense that they are based on a synoptic-scale experience of the analyst and a set of calibration parameters (Scherrer et al. 2006). Scaife et al. (2010) have pointed out that daily or sub-daily data of the mean 500-hPa geopotential height are the most useful variables to identify atmospheric blocking. On this basis, some indices have been proposed based on the determination of major positive height anomalies (Dole and Gordon 1983), on positive latitudinal gradients of the geopotential height (Lejenäs and Økland 1983; Tibaldi and Molteni 1990; Wiedenmann et al. 2002), on potential vorticity (PV) framework (Schwierz et al. 2004) and on the degree of splitting of westerly airstreams (Marshall et al. 2013).

3 Data and methods

3.1 Study area

The present study covers the central region of Middle East between 22° and 42° N latitude and 37°–67° E longitude and elevation values from − 75 to 5415 m a.s.l (Fig. 3). A wide belt of seismicity results from a complex plate tectonic interplay that includes subduction zones, transform faulting, compressional and crustal extensions taking place between four major plates: Arabia, Eurasia, India, and Africa, together with the smaller tectonic block of Anatolia (Mansouri Daneshvar et al. 2014a). Based on the gridded world climate data (Hijmans et al. 2005), the mean values of annual temperature and precipitation are 16–20 °C and 200–400 mm, respectively (Fig. 4). Hence, the region is classified as part of the arid and semi-arid belt. Major contributions to the regional rainfall come from Mediterranean airflows. Blocking events arise from westerly

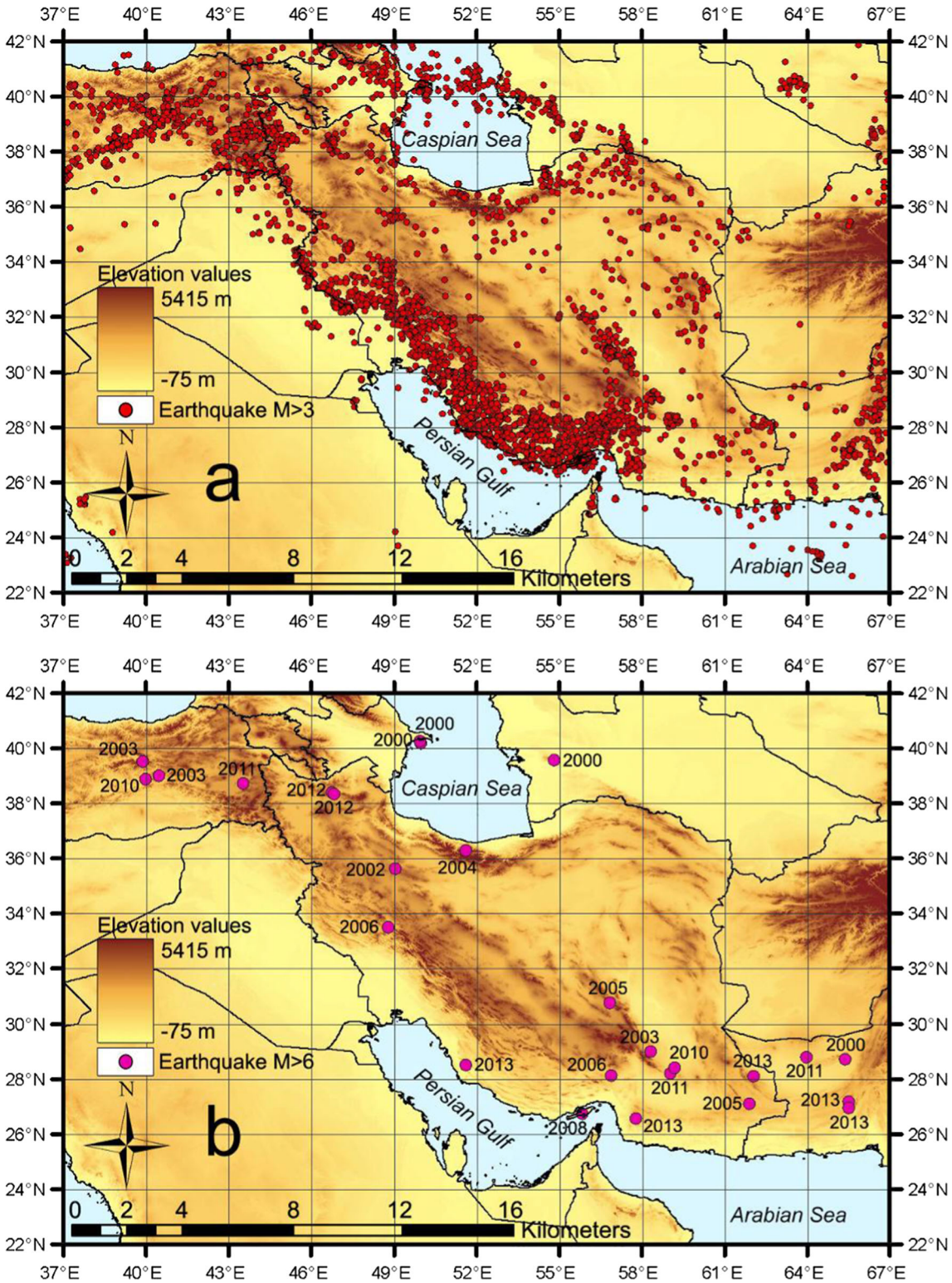

Fig. 3 Topographic map of the study area, together with **a** 3970-earthquake epicenters of M > 3 events; and **b** 26-earthquake epicenters of M > 6 events for the period 2000–2013

winds. These blocking events are usually of the dipole type, linked to blocked high-pressure areas over central Asia and intersected by low-pressure areas along the tectonically active regions in the seismic belt.

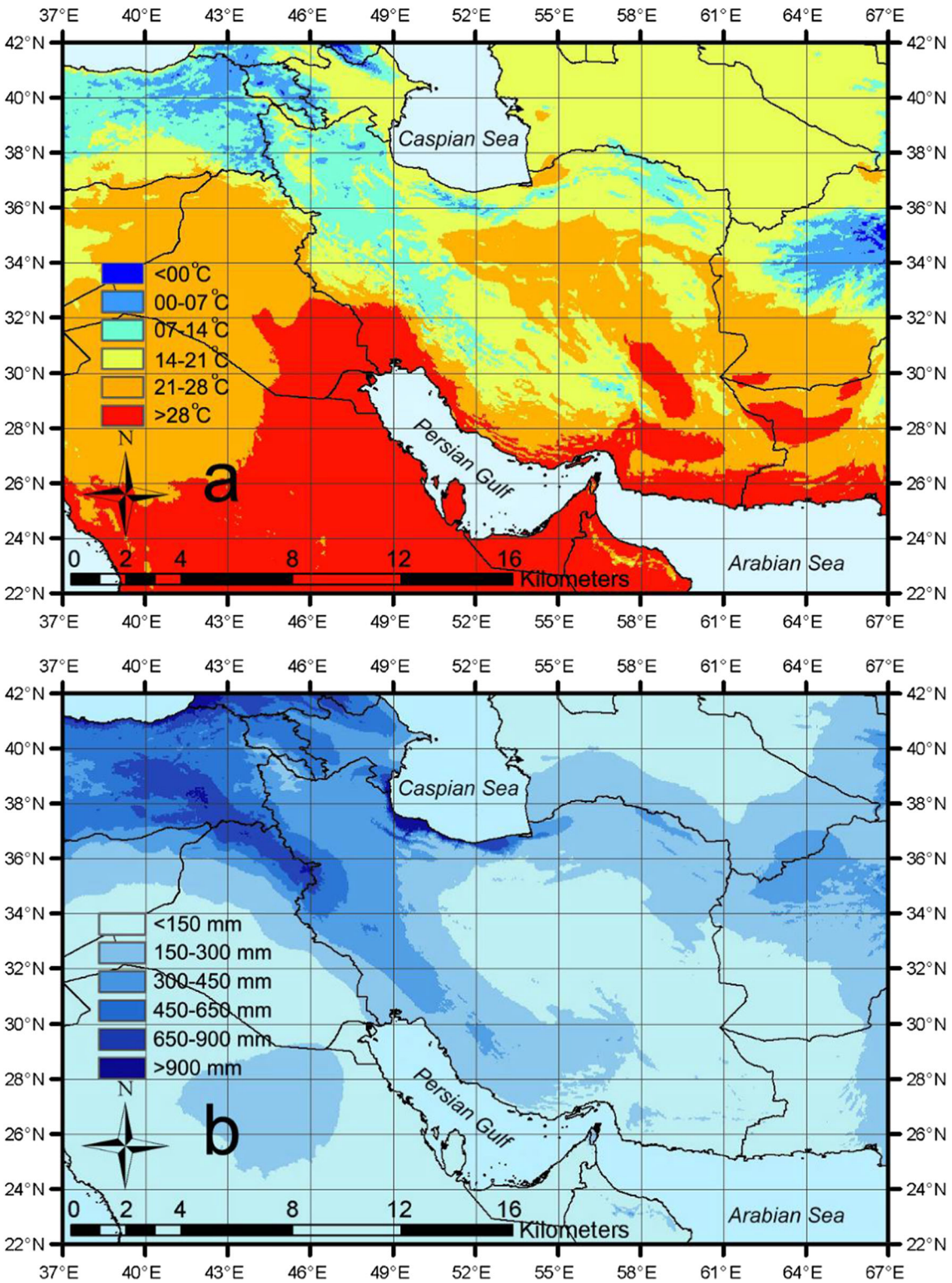

Fig. 4 The gridded climatic maps of **a:** mean annual temperature; and **b:** precipitation in the study area

Table 1 Seismo-climatic properties and indices before and after blocking episodes

No.	Blocking event properties				14-day seismicity before blocking episode			14-day seismicity after blocking episode			Seismo-climatic index
	Time period	Genesis longitude	Wiedenmann index	Selected episode	Earthquake frequency	Mean magnitude	Maximum magnitude	Earthquake frequency	Mean magnitude	Maximum magnitude	
1	2000/01/21–2000/01/26	70	4.17	2000/01/25	2	4.1	4.6	6	4.5	5.3	3.29
2	2000/04/28–2000/05/03	15	2.32	2000/05/03	2	3.8	4.1	9	4.3	5.1	5.09
3	2000/05/12–2000/05/18	65	2.17	2000/05/03	4	4.2	4.5	8	4.0	4.4	1.90
4	2000/10/06–2000/10/14	40	2.30	2000/10/18	2	4.6	4.7	5	4.2	5.3	2.28
5	2000/10/16–2000/10/21	25	3.19	2000/10/21	2	4.7	4.7	5	4.2	5.3	2.23
6	2000/11/06–2000/11/11	45	2.70	2000/11/11	3	4.2	4.9	17	4.6	6.8	6.21
7	2001/04/24–2001/05/06	50	2.39	2001/05/06	2	4.2	4.2	5	4.2	4.5	2.50
8	2001/07/09–2001/07/23	35	2.63	2001/07/23	2	4.0	4.0	2	4.2	4.2	1.05
9	2001/10/15–2001/10/25	10	3.33	2001/10/16	3	4.3	4.9	5	4.5	4.6	1.74
10	2001/11/28–2001/12/01	50	3.12	2001/11/29	8	4.1	5.0	10	4.4	4.7	1.34
11	2002/04/02–2002/04/08	15	2.37	2002/04/08	10	4.4	5.2	12	4.3	5.3	1.17
12	2002/04/25–2002/05/05	30	2.60	2002/04/25	7	4.4	5.3	20	4.4	5.4	2.86
13	2002/05/23–2002/06/01	30	3.46	2002/06/01	7	4.2	4.7	13	4.3	5.0	1.90
14	2002/06/03–2002/06/13	20	2.43	2002/06/13	7	4.0	4.5	21	4.5	6.5	3.38
15	2002/07/30–2002/08/08	50	2.56	2002/07/30	4	4.1	4.5	5	4.2	4.4	1.28
16	2002/08/15–2002/08/28	20	2.37	2002/08/24	7	4.2	4.4	10	4.3	5.2	1.46
17	2002/12/26–2003/01/28	10	4.30	2002/12/30	2	4.9	5.2	10	4.5	4.8	4.59
18	2003/02/06–2003/02/11	50	3.15	2003/02/11	1	4.6	4.6	3	4.6	5.6	3.00
19	2003/02/11–2003/02/28	10	4.79	2003/02/27	2	4.2	4.2	9	4.4	4.7	4.71
20	2003/04/02–2003/04/07	60	3.14	2003/04/07	3	4.3	4.6	3	4.3	4.6	1.00
21	2003/04/15–2003/04/24	10	4.22	2003/04/24	2	4.3	4.5	12	4.3	6.4	6.00
22	2003/06/01–2003/06/10	10	2.27	2003/06/10	4	4.3	4.7	3	4.0	4.5	0.70
23	2003/11/01–2003/11/06	50	2.95	2003/11/06	4	4.7	5.0	7	4.4	4.8	1.64
24	2003/11/05–2003/11/16	10	4.21	2003/11/16	4	4.5	4.7	11	4.6	5.1	2.81
25	2003/11/27–2003/12/04	30	3.51	2003/12/04	6	4.3	4.7	3	4.4	5.0	0.51
26	2003/12/16–2003/12/21	70	2.15	2003/12/18	4	4.6	5.1	28	4.3	6.6	6.54
27	2003/12/28–2004/01/05	30	2.20	2004/01/05	13	3.6	4.6	21	4.2	5.2	1.88
28	2004/01/14–2004/01/20	70	3.07	2004/01/18	7	4.2	5.2	11	4.4	5.2	1.65
29	2004/04/14–2004/04/22	10	2.31	2004/04/08	5	4.1	4.3	5	4.5	4.6	1.10
30	2004/04/29–2004/05/08	10	3.11	2004/05/08	4	4.3	4.6	6	4.2	5.0	1.47
31	2004/05/12–2004/05/23	70	3.13	2004/05/20	5	4.0	4.4	34	3.9	6.3	6.63
32	2004/06/25–2004/07/12	60	2.01	2004/07/12	6	4.3	5.1	15	4.1	5.1	2.38
33	2004/07/12–2004/07/24	50	2.31	2004/07/14	4	4.0	4.5	13	4.1	5.1	3.33
34	2004/07/26–2004/08/10	50	2.47	2004/07/30	7	4.2	5.1	14	4.3	5.0	2.05

Table 1 (continued)

No.	Blocking event properties				14-day seismicity before blocking episode			14-day seismicity after blocking episode			Seismo-climatic index
	Time period	Genesis longitude	Wiedenmann index	Selected episode	Earthquake frequency	Mean magnitude	Maximum magnitude	Earthquake frequency	Mean magnitude	Maximum magnitude	
35	2004/08/27–2004/09/15	30	2.91	2004/08/31	7	4.1	4.7	11	4.3	4.7	1.65
36	2004/11/02–2004/11/13	20	2.24	2004/11/06	5	3.9	4.9	17	3.9	4.7	3.40
37	2004/11/21–2004/11/26	70	3.56	2004/11/21	9	4.1	4.8	21	4.0	5.2	2.28
38	2005/02/18–2005/03/18	30	3.46	2005/02/22	5	3.6	4.6	30	4.0	6.4	6.67
39	2005/05/10–2005/05/25	60	2.96	2005/05/12	8	3.7	4.9	15	4.2	5.2	2.13
40	2005/08/05–2005/08/14	40	2.41	2005/08/07	8	3.8	4.4	12	4.1	5.1	1.62
41	2005/08/18–2005/09/01	10	2.72	2005/08/28	6	4.2	4.6	9	4.2	4.8	1.50
42	2005/09/17–2005/09/23	70	2.16	2005/09/23	5	4.2	4.7	7	4.4	5.2	1.47
43	2005/10/04–2005/10/16	10	3.95	2005/09/23	2	4.0	4.2	3	4.1	4.7	1.54
44	2005/11/17–2005/11/23	60	3.24	2005/11/18	8	3.8	4.5	28	4.3	5.9	3.96
45	2005/11/27–2005/12/07	10	3.09	2005/11/27	8	4.3	5.1	30	4.3	5.9	3.75
46	2005/12/18–2005/12/23	70	4.32	2005/12/23	4	3.8	4.1	23	3.7	5.0	5.60
47	2006/05/30–2006/06/10	30	3.67	2006/06/03	8	3.7	4.2	17	4.0	5.1	2.30
48	2006/06/18–2006/06/25	30	2.40	2006/06/23	7	3.7	4.4	26	4.0	5.8	4.02
49	2006/09/06–2006/09/11	70	2.33	2006/09/10	3	4.0	4.8	15	4.0	5.0	5.00
50	2006/09/10–2006/09/18	10	2.88	2006/09/14	10	4.0	5.0	18	3.8	4.9	1.71
51	2006/09/21–2006/09/28	10	2.55	2006/09/23	11	4.0	4.9	15	3.8	4.9	1.30
52	2006/10/09–2006/10/20	10	2.64	2006/10/17	8	4.3	5.3	13	3.9	4.6	1.47
53	2006/11/26–2006/12/06	20	3.15	2006/12/06	6	3.9	4.4	11	4.0	4.8	1.88
54	2007/03/20–2007/03/31	40	3.80	2007/03/24	11	4.2	5.7	12	3.9	5.0	1.01
55	2007/04/18–2007/04/24	60	3.37	2007/04/20	6	4.2	4.6	26	4.1	5.2	4.23
56	2007/04/25–2007/05/05	10	3.10	2007/04/25	14	3.9	4.6	19	4.2	5.2	1.46
57	2007/07/02–2007/07/08	60	2.18	2007/07/08	5	4.1	5.0	5	4.3	5.2	1.05
58	2007/07/11–2007/07/18	70	2.49	2007/07/16	4	4.0	5.2	6	4.2	5.0	1.58
59	2007/08/05–2007/08/11	20	2.63	2007/08/08	3	4.1	4.4	9	4.1	4.7	3.00
60	2007/08/16–2007/08/22	50	2.22	2007/08/20	8	4.1	4.8	18	4.2	5.3	2.30
61	2007/10/24–2007/11/13	20	2.30	2007/11/08	4	4.1	4.4	8	4.1	4.7	2.00
62	2007/12/04–2007/12/14	50	2.78	2007/12/09	7	3.7	4.3	12	3.7	4.6	1.71
63	2007/12/26–2008/01/01	50	2.52	2007/12/29	8	3.8	4.4	11	3.8	4.6	1.38
64	2008/01/14–2008/01/23	30	2.29	2008/01/23	6	4.0	4.5	17	3.9	4.9	2.76
65	2008/01/31–2008/02/09	10	5.99	2008/01/31	12	3.9	4.4	14	3.9	4.9	1.17
66	2008/03/26–2008/04/01	60	3.04	2008/03/26	11	4.0	4.8	9	4.0	4.8	0.82
67	2008/04/03–2008/04/11	40	2.29	2008/04/11	4	3.7	4.0	10	3.9	4.7	2.64
68	2008/05/27–2008/06/15	20	2.69	2008/06/15	3	3.8	4.1	17	3.9	4.6	5.82

Table 1 (continued)

No.	Blocking event properties				14-day seismicity before blocking episode			14-day seismicity after blocking episode			Seismo-climatic index
	Time period	Genesis longitude	Wiedenmann index	Selected episode	Earthquake frequency	Mean magnitude	Maximum magnitude	Earthquake frequency	Mean magnitude	Maximum magnitude	
69	2008/06/29–2008/07/08	20	3.30	2008/07/08	7	4.0	5.2	15	3.9	4.6	2.09
70	2008/07/02–2008/07/10	20	2.44	2008/07/10	6	4.1	5.2	15	3.8	4.6	2.32
71	2008/10/26–2008/11/03	40	3.02	2008/11/03	21	4.1	5.4	13	3.8	4.9	0.57
72	2008/12/12–2008/12/20	30	2.62	2008/12/20	5	3.9	4.4	11	4.3	5.8	2.43
73	2009/01/29–2009/02/03	10	3.96	2009/01/29	1	4.1	4.1	3	4.4	5.1	3.22
74	2009/02/15–2009/02/27	50	3.59	2009/02/27	3	4.8	5.1	3	4.4	4.7	0.92
75	2009/04/09–2009/04/21	20	2.88	2009/04/25	3	4.3	4.7	5	4.4	4.6	1.71
76	2009/04/23–2009/05/03	10	3.49	2009/05/03	3	4.7	5.2	6	4.4	5.0	1.87
77	2009/06/11–2009/06/19	50	2.28	2009/06/03	1	3.8	3.8	3	4.5	4.9	3.55
78	2009/07/23–2009/08/02	60	2.02	2009/08/02	3	4.8	5.3	3	4.3	4.5	0.90
79	2009/08/03–2009/08/12	20	2.04	2009/08/12	3	4.3	4.5	3	4.3	4.7	1.00
80	2009/11/12–2009/11/20	50	2.76	2009/11/13	2	4.5	5.0	3	4.5	4.9	1.50
81	2009/11/31–2009/12/10	20	3.76	2009/12/10	1	4.4	4.4	3	4.7	4.9	3.20
82	2009/12/01–2009/12/11	40	3.00	2009/12/11	1	4.6	4.6	2	4.8	4.9	2.09
83	2010/01/04–2010/01/18	70	2.34	2010/01/10	2	4.9	5.0	10	4.5	5.0	4.59
84	2010/02/01–2010/02/07	50	3.25	2010/02/07	3	4.6	4.9	5	4.3	4.6	1.56
85	2010/02/09–2010/02/14	50	3.38	2010/02/14	4	4.4	4.6	6	4.6	5.2	1.57
86	2010/04/19–2010/04/26	70	2.68	2010/04/19	3	4.5	4.7	5	4.5	5.0	1.67
87	2010/04/29–2010/05/11	60	2.76	2010/05/11	1	4.0	4.0	5	4.4	5.1	5.50
88	2010/05/02–2010/05/24	40	3.08	2010/05/24	3	4.0	4.1	5	4.4	4.8	1.83
89	2010/07/04–2010/07/30	20	2.44	2010/07/20	3	4.2	4.5	7	4.9	5.8	2.72
90	2010/08/31–2010/09/16	45	2.50	2010/09/08	4	4.7	5.2	6	4.3	4.7	1.37
91	2010/10/09–2010/10/19	10	3.83	2010/10/19	2	4.4	4.6	6	4.4	4.6	3.00
92	2010/11/29–2010/12/04	20	2.03	2010/11/29	6	4.3	5.5	3	4.5	4.9	0.52
93	2010/12/11–2010/12/16	70	4.69	2010/12/16	2	4.4	4.8	12	4.5	6.7	6.14
94	2010/12/19–2011/01/22	10	4.73	2011/01/18	2	4.6	5.1	18	4.7	7.2	9.20
95	2011/03/01–2011/03/09	20	4.46	2011/03/09	5	4.6	5.3	7	4.3	4.8	1.31
96	2011/03/16–2011/03/23	20	4.38	2011/03/23	10	4.3	4.8	9	4.1	4.6	0.86
97	2011/05/04–2011/05/12	40	2.77	2011/05/08	2	4.1	4.1	4	4.5	4.9	2.20
98	2011/06/22–2011/07/02	50	2.27	2011/07/01	4	4.6	5.2	5	4.2	4.4	1.14
99	2011/07/20–2011/07/27	50	2.40	2011/07/27	5	4.5	5.0	9	4.3	4.8	1.72
100	2011/08/17–2011/08/24	30	2.13	2011/08/24	2	4.4	4.9	5	4.4	4.7	2.50
101	2011/09/08–2011/09/21	50	2.95	2011/09/21	3	4.4	4.6	6	4.3	5.5	1.95
102	2011/09/28–2011/10/03	10	3.65	2011/10/03	5	4.1	4.3	4	4.3	4.9	0.84

Table 1 (continued)

No.	Blocking event properties				14-day seismicity before blocking episode			14-day seismicity after blocking episode			Seismo-climatic index
	Time period	Genesis longitude	Wiedenmann index	Selected episode	Earthquake frequency	Mean magnitude	Maximum magnitude	Earthquake frequency	Mean magnitude	Maximum magnitude	
103	2011/10/08–2011/10/16	50	2.26	2011/10/11	2	4.1	4.2	7	4.6	5.2	3.93
104	2011/10/22–2011/10/29	20	3.38	2011/10/22	5	4.6	5.2	118	4.4	7.1	22.57
105	2011/11/30–2011/12/20	20	3.99	2011/12/08	6	4.6	4.9	11	4.3	4.9	1.71
106	2012/01/06–2012/01/12	60	3.69	2012/01/11	7	4.6	5.2	11	4.5	5.1	1.54
107	2012/01/17–2012/01/29	60	3.61	2012/01/17	9	4.5	5.2	6	4.4	5.1	0.65
108	2012/02/11–2012/02/20	60	3.02	2012/02/20	4	4.6	4.7	9	4.5	5.2	2.20
109	2012/02/31–2012/03/09	70	4.58	2012/03/09	6	4.5	5.1	9	4.4	4.7	1.47
110	2012/04/13–2012/04/19	60	2.86	2012/04/18	6	4.2	4.6	33	4.5	5.1	5.89
111	2012/04/27–2012/05/02	30	3.15	2012/05/02	9	4.4	4.7	15	4.5	5.6	1.70
112	2012/05/15–2012/05/22	50	2.68	2012/05/18	13	4.3	5.1	9	4.4	5.1	0.71
113	2012/07/17–2012/08/03	70	2.57	2012/08/02	5	4.5	5.2	30	4.5	6.4	6.00
114	2012/12/08–2012/12/20	50	3.68	2012/12/20	2	4.3	4.5	3	4.8	5.2	1.67
115	2013/02/01–2013/02/08	70	2.89	2013/02/08	2	4.4	4.5	4	4.1	4.4	1.86
116	2013/02/08–2013/02/14	50	3.52	2013/02/12	2	4.4	4.5	6	4.1	4.4	2.80
117	2013/04/02–2013/04/08	60	2.76	2013/04/08	3	4.2	4.5	63	4.5	7.8	22.50
118	2013/05/06–2013/05/23	30	2.51	2013/05/11	13	4.4	5.2	55	4.5	6.1	4.33
119	2013/05/25–2013/06/07	50	3.36	2013/05/31	4	4.6	5.2	6	4.2	4.6	1.37
120	2013/06/21–2013/07/05	60	2.72	2013/06/21	2	4.3	4.5	5	4.2	4.3	2.44
121	2013/09/06–2013/09/21	20	2.51	2013/09/21	9	4.3	5.0	51	4.6	7.7	6.06
–	Mean values	–	3.00	–	5	4.23	4.72	13	4.27	5.13	2.88

3.2 Data preparation

In the present study, about 121 blocking events (BI > 2)[2] were compiled according to the northern hemisphere blocking archive via (http://weather.missouri.edu/gcc) as shown in Table 1 (Lupo et al. 2014), covering the period 2000-2013 and the longitude range from 10°E to 70°E. All blocking events are listed by longitude, start and end date, number of days and blocking index. A number of different indices have been proposed and used to diagnose atmospheric blocking (e.g., Rex 1950; Lejenäs and Økland 1983; Tibaldi and Molteni 1990; Wiedenmann et al. 2002; Pelly and Hoskins 2003; Berrisford et al. 2007). Scaife et al. (2010) pointed out that, when these indices are applied to numerical models, the models underestimate the blocking frequency (e.g., D'Andrea et al. 1998).

Among the aforementioned indices, the archive of the source of blocking data has applied the Blocking Index (BI) proposed by Wiedenmann et al. (2002). The BI values were calculated by normalizing the central high-pressure value using subjectively determined geopotential contour lines. They were then scaled from 1 to 10. BI can be used as a diagnostic tool for examining the relative strength of large-scale flow regimes within blocking regions. According to Wiedenmann et al. (2002), classifying of the BI intensity for blocking events in the Northern Hemisphere (NH) can be described as weak (BI > 2.0), moderate (2.0 < BI < 4.3) or strong (BI > 4.3). During the time window covered by this study, 3970 earthquake events (M > 3)[3] were analyzed, obtained from the earthquake archive at http://earthquake.usgs.gov/earthquakes, including 26 major earthquakes (M > 6) as shown in Fig. 3 (USGS 2014).

Decades ago, Gutenberg and Richter (1954)[4] have made attempts to statistically correlate earthquake frequencies and magnitudes. Recent studies use linear or logistic indicators for a probabilistic assessment of temporal and spatial variations of seismic activity (Thompson et al. 2007), for quantifying of aftershock activity (Enescu et al. 2007), for an analysis between sea surface temperature and seismicity (Molchanov 2010) and for an analysis of rain-induced seismicity (Dinske and Shapiro 2013). Using a range of parameters (Mansouri Daneshvar 2015), which provide short-term links between blocking events and earthquakes, the present study proposes a new seismo-climatic index (SCI) based on variations of earthquake frequency and magnitude before and after blocking events:

$$SCI = (FeqA \times MeqA)/(FeqB \times MeqB), \quad (1)$$

where *SCI* is the seismo-climatic index, *FeqA* is the earthquake frequency within a 2-week period after the selected blocking episode, *MeqA* is the mean magnitude of earthquakes within 2-week after the selected blocking episode, *FeqB* is the earthquake frequency within a 2-week period before the selected blocking episode, and *MeqB* is the mean magnitude of earthquakes within the 2-week period before the selected blocking episode. In this study, selected blocking episode depends on any day during the blocking event's time-period that includes at least one earthquake in the study area (central region of the Middle East). Selection of a blocking episode (day) depends on the persistence of the atmospheric blocking event across a given study area (central region of the Middle East), outlined by the earthquakes' epicenters. Therefore, the spread of selected blocking episode days from the middle of blocking event ranges from − 13 days to 17 days. This confirms that a 2-week time window after and before the selected blocking episode is a reasonable time window to correlate with earthquake occurrences.

In this regard, SCI is defined as a ratio of the multiple frequencies and mean magnitude of earthquakes within 2-week after and before the selected blocking episode. Hence, based on the standard deviation of SCI values, the threshold of significant relation for SCI values is found to be 3. Therefore, SCI values > 3 denote a possible relationship between blocking events and a subsequent seismicity. For example, an SCI value of 3 indicates that the seismic activity after a blocking episode in the area under study increases by a factor of 3. Accordingly, to define the relationship between blocking events on one-hand and earthquake frequencies and magnitudes on the other hand, the Pearson correlation coefficients were calculated for the time series in SPSS.

4 Result and discussion

4.1 Statistical analysis

The cataloged data from global archives were first tabulated as daily time series to illustrate possible correlations. According to Eq. 1, all blocking events were then compiled as listed in Table 1, together with seismo-climatic indicators and indices. The resulting SCI values range from 0.51 to 22.57. The mean value of SCI is 2.88, indicating that the probability of an atmospheric blocking event preceding an earthquake is higher by a factor of nearly three than the longtime average. The means and maxima of earthquake magnitudes and frequencies before selected blocking episodes were 4.23, 4.73 and 5, respectively. After blocking

[2] Blocking index over than 2 based on Wiedenmann et al. (2002).

[3] . Earthquake magnitude over than 3 based on Richter (1958).

[4] $\log_{10}N = a - bM$, where M is magnitude, N is frequency, a and b are constants (Gutenberg and Richter 1954).

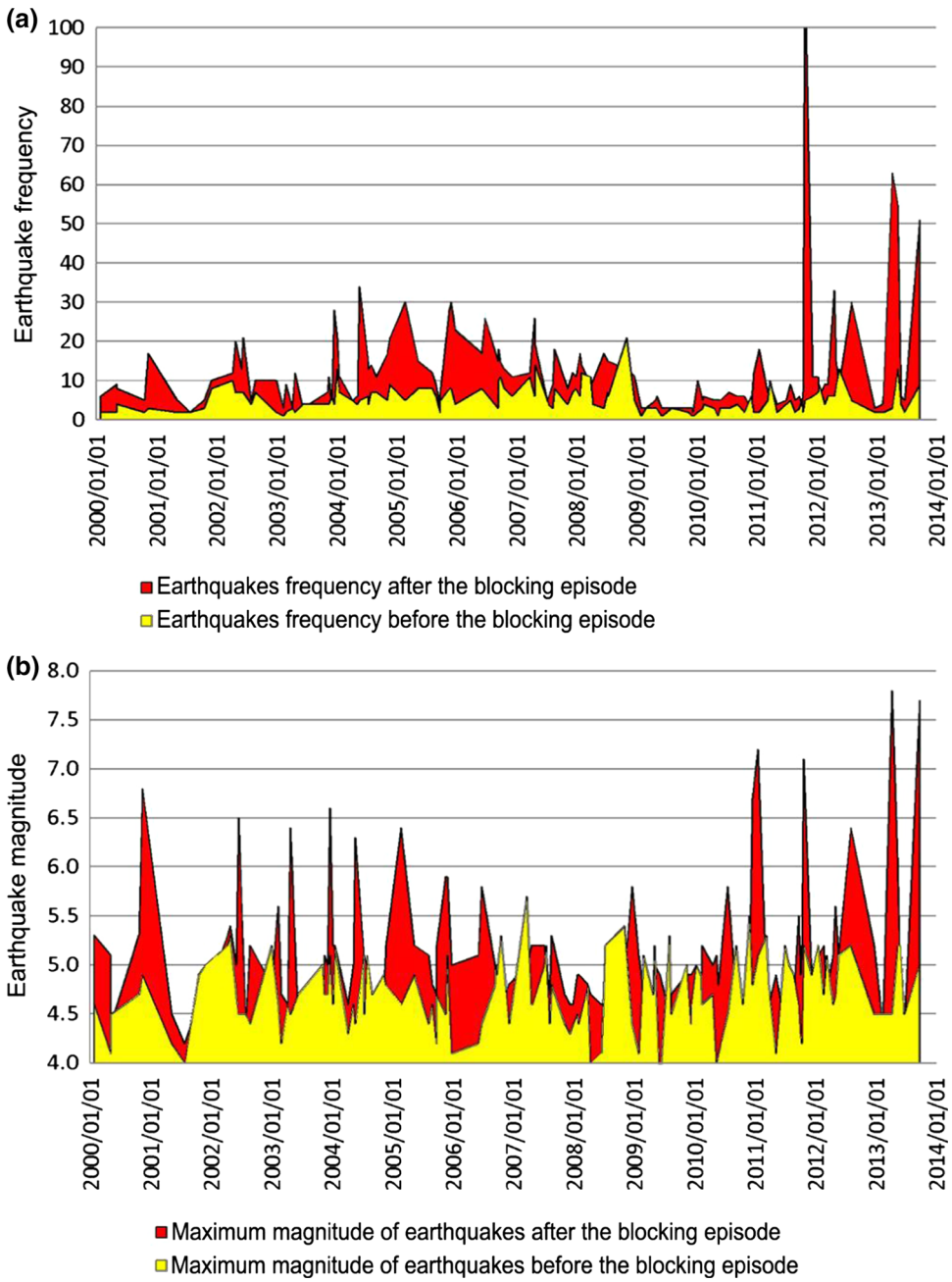

Fig. 5 The relations between **a** blocking episodes and earthquake frequencies; **b** blocking episodes and maximum magnitude of earthquakes

events, the means and maxima of earthquake magnitude and frequency increased to 4.27, 5.13, and 13, respectively. Hence, seismicity in the Middle East during 2000–2013 tends to be preceded and followed by atmospheric blocking events relative to the longtime average. Consequently, high SCI values denote an increased probability of earthquakes. Table 1 shows two particularly high SCI values (> 20) correlated to two major earthquake swarms (M > 7).[5] The relation between blocking events, seismic frequency, and magnitude of earthquakes is presented in Fig. 5, which also suggests an increase in the number of earthquakes within a 2-week period after blocking events.

Pearson correlation coefficients were applied to illustrate the significance between blocking events and seismicity increase over the subsequent 2-week period. The correlation coefficients between SCI values, seismic frequency and magnitudes of the earthquakes are 0.694 ($R2 = 0.48$, $P < 0.05$) and 0.803 ($R2 = 0.64$, $P < 0.05$), respectively (Table 2). Except for the correlation between SCI and mean magnitudes, these correlation coefficients

[5] The earthquake swarms in 2011 and 2013 include about 118 and 63 seismic events after the blocking events, respectively. These anomalous events, which are controlled by the regional tectonic and geological indicators, deserve to be evaluated in further studies.

Table 2 The correlation between seismo-climatic index and earthquake characteristics for 14-day seismicity after selected blocking episodes

Earthquake characteristics	Test	Seismo-climatic index
Frequency	Correlation*	0.803
	R^2	0.645
	Sig.	0.000
Mean magnitude	Correlation*	0.152
	R^2	0.023
	Sig.	0.097
Maximum magnitude	Correlation*	0.694
	R^2	0.482
	Sig.	0.000

*Correlation is significant at the 0.05 level (two-tailed)

indicate the strong correlation between blocking events on one side and seismic events and their magnitudes on the other side. This may provide a basis for improved short-term forecasting of major earthquakes and seismic swarms.

For instance, for SCI > 6 during 2000–2013, at least 16 out of 26 major earthquakes (M > 6) are identified (∼ 62%) as occurring within 14 days after blocking events in the area of the future epicenters. Mansouri Daneshvar et al. (2015) proposed that, if anomalies associated with blocking events such as cyclogenesis, thunderstorm, and low-pressure persistence occur within days and weeks before main seismic events, it is justified to consider them earthquake precursors. This time window, classified as short-term, agrees with previous electromagnetic and atmospheric studies of earthquake precursors (Ouzounov et al. 2007; Cicerone et al. 2009). The physical process appears to be linked to the waxing and waning of tectonic stresses along the fault segments under consideration (Sykes et al. 1999). Episodes of stress-induced massive air ionization at ground level before major earthquakes, either days or weeks before the event, appear to occur as a result of stress pulses, which lead to air ionization at the Earth's surface (Freund et al. 2009). However, not every build-up of stress will lead to rupture (Freund 2013; Heraud 2014). Thus, there will certainly be episodes when stresses are sufficient to induce air ionization at the Earth's surface but they then relax without causing a major seismic event.

In wider temporal intervals, the data indicate that, by assuming SCI > 6, 73% of the M > 6 earthquakes (19 out of 26) occurred within 3–4 weeks after blocking events (within ∼ 5 weeks after the on-set of blocking event) over the respective epicentral areas (Table 3). The mean SCI value is 9.5, indicating that the major earthquake activity

Table 3 Major earthquakes (M > 6) in the Middle East from 2000 to 2013 preceded by blocking episodes

No.	Blocking event properties				Seismo-climatic index	Major earthquake characteristics	
	Time period	Genesis longitude	Wiedenmann index	Selected episode		Date	Magnitude
1	2000/11/06–2000/11/11	45	2.70	2000/11/11	6.21	2000/11/25	6.8
						2000/11/25	6.5
						2000/12/06	7.0
2	2003/04/15–2003/04/24	10	4.22	2003/04/24	6.00	2003/05/01	6.4
3	2003/12/16–2003/12/21	70	2.15	2003/12/18	6.54	2003/12/26	6.6
4	2004/05/12–2004/05/23	70	3.13	2004/05/17	6.63	2004/05/28	6.3
5	2005/02/18–2005/03/18	30	3.46	2005/02/22	6.67	2005/02/22	6.4
						2005/03/13	6.0
6	2010/12/11–2010/12/16	70	4.69	2010/12/16	6.14	2010/12/20	6.7
7	2010/12/19–2011/01/22	10	4.73	2011/01/18	9.20	2011/01/18	7.2
						2011/01/27	6.2
8	2011/10/20–2011/10/29	20	3.38	2011/10/20	22.57	2011/10/23	7.1
9	2012/07/17–2012/08/03	70	2.57	2012/08/02	6.00	2012/08/11	6.4
						2012/08/11	6.2
10	2013/04/02–2013/04/08	60	2.76	2013/04/08	22.50	2013/04/09	6.4
						2013/04/16	7.8
						2013/05/13	6.1
11	2013/09/06–2013/09/21	20	2.51	2013/09/21	6.06	2013/09/24	7.7
						2013/09/28	6.8
–	Mean values	–	3.3	–	9.5	–	6.6

can increase nearly tenfold after blocking events. In a recent paper, Mansouri Daneshvar and Freund (2017) documented that the spatiotemporal characteristics of atmospheric and ionospheric anomalies before the Illapel earthquake in Chile also co-registered within 3–5 weeks.

4.2 Conceptual description

We propose that persistent low-pressure, cyclogenesis, thunderstorm activity, convective clouds and air turbulence before major earthquakes, as parts of blocking events, are caused or triggered by tectonic stresses within the Earth's crust, which lead to the activation of positive electronic charge carriers in the hypocentral rock volume propagating through the crust, accumulate at the Earth's surface and cause field-ionization of air molecules and corona discharges (Freund et al. 2009). Field-ionization and corona discharges generate predominantly positive air ions and mixtures of positive and negative air ions, respectively. Freund (2013) argued that, since the number density of stress-activated positive-hole charge carriers in the rocks increases before major earthquakes, the negative charge at the underside of thunderclouds will tend to attract more positive charges in the Earth's surface below thunderclouds. The accumulation of these positive charges amplifies the field ionization of air molecules at the Earth's surface and generates more positive airborne ions, which rise upward in the prevailing electric field, acting as leaders to which downward lightning strikes can connect. The lightning strikes in turn deliver electrons to the ground, which compensate for the accumulated positive charges. Naturally, the thundercloud electric field has an electric field high enough to trigger coronal discharges at the Earth's surface initiating lightning strikes (Bazelyan et al. 2009). Air ionization and coronal discharges are processes that are triggered at the nanometer scale. 30 kV/cm translate into 3 V/μm and 3 mV/nm. The controlling physical entity is not the E field but the potential V. Note that the E field is, by definition, the potential V divided by the distance d: E = V/d. Experimentally, only the value of V is readily accessible. Values are given by Freund et al. (2009) amount up to 3 V. Such values easily create E fields approximately many kilo V/μm and Mega V/nm. Plenty to generate electric discharges even over centimeter distances.

Conversely, the positive tops of thunderclouds become even more positive, generating positive ions, mostly O^+, which rise upward towards the ionosphere causing perturbations in the electron distribution in the ionospheric plasma through electrostatic interactions. This sequence of processes in the Earth's crust and at the Earth's surface provides an explanation why, before major seismic activity, the number of downward lightning strikes increases relative to the number of cloud-to-cloud lightning discharges (Liu et al. 2015).

The increased frequency of downward lightning strikes prior to major earthquakes is consistent with the conclusion drawn from other studies (Freund et al. 2009; Freund 2013) that the build-up of tectonic stresses deep in the crust leads to the activation of positive hole charge carriers, which spread out into the surrounding crust. Upon reaching the Earth's surface, the positive holes accumulate, causing positive air ionization, the formation of cluster ions and moisture condensation. Moisture condensation releases latent heat, which will produce thermal updrafts, which in turn lead to low-pressure conditions and the possibility of bifurcation and atmospheric blocking. In this scenario, the build-up of positive surface charges is not initiated from above by charges due to thunderstorm activity but driven from within the Earth's crust.

Positive holes have the remarkable ability to flow out of the stressed rock volume into and through the surrounding less stressed and unstressed rocks, traveling fast and far. When they reach the Earth's surface, they accumulate over a wide area, setting up microscopic but steep electric fields at the ground-to-air interface (Freund 2013). Laboratory experiments have demonstrated that the positive surface charge leads first to field ionization of air molecules, producing positive airborne ions, followed by corona discharges, which produce airborne ions of either polarity plus an abundance of free electrons. As a result, the sign of the surface charge changes abruptly from positive to negative (Freund et al. 2009).

Accumulation of blocking-related atmospheric anomalies such as cyclogenesis increased cloud formation, and anomalous rainfall before major earthquakes is consistent with this overall concept. Hence, atmospheric blocking events in a seismological region may be categorized as a potential pre-earthquake phenomenon.

5 Conclusion

In the present study, the broad temporal and spatial correlations between atmospheric blocking and seismicity were investigated introducing a new seismo-climatic index (SCI) and using data from two global archives of USGS and University of Missouri.

The results indicate that application of the SCI forecasts 62–73% seismic events in the study area occurring within 14–33 days after the on-set of a blocking event. SCI values > 6 indicate a strong correlation between blocking events and seismicity including a series of major earthquakes ($M > 6$). The present study statistically confirms that, as suggested earlier (Mansouri Daneshvar et al. 2015), blocking events are precursory indicators of seismic activity.

The present study also reaffirms a process, by which tectonic stresses deep in the Earth's crust lead to positive charges at the surface-to-air interface and air ionization, which can trigger atmospheric blocks such as persistent low-pressure areas, cyclogenesis, cloud coverage, and anomalous rainfall before the major earthquakes. Hence, atmospheric blocking events in a seismically active region can be categorized as a pre-earthquake phenomenon. More research based on the physical and dynamical reactions between the Earth's crust and atmosphere will be needed to substantiate this model and add further refinements.

Acknowledgements M.R. Mansouri-Daneshvar likes to dedicate the present paper to his late dear mother Aghdas Nasle-Saraji for her never-failing support and to Somayeh Rezayi and Artina Mansouri-Daneshvar for their precious help during data preparation. The authors are grateful to the anonymous reviewers for their insightful comments on the data interpretations. Furthermore, the authors would like to thank the handling editor Dr. Stefan Schmid for his valuable technical suggestions and practical considerations on the paper from its submission to the publication process.

Funding This study was not funded by any grant.

Compliance with ethical standards

Conflict of interest The authors declare that they have no conflict of interest.

Ethical approval This article does not contain any studies with participants performed by any of the authors.

Informed consent Informed consent was obtained from individual participant included in the study.

References

Bazelyan, E. M., Raizer, Y. P., Aleksandrov, N. L., & D'Alessandro, F. (2009). Corona processes and lightning attachment: The effect of wind during thunderstorms. *Atmospheric Research, 94,* 436–447.

Berrisford, P. B., Hoskins, J., & Tyrlis, E. (2007). Blocking and Rossby wave breaking on the dynamical tropopause in the Southern Hemisphere. *Journal of the Atmospheric Sciences, 64,* 2881–2898.

Bleier, T., Dunson, C., Maniscalco, M., Bryant, N., Bambery, R., & Freund, F. T. (2009). Investigation of ULF magnetic pulsations, air conductivity changes, and infra red signatures associated with the 30 October Alum Rock M5.4 earthquake. *Natural Hazards and Earth System Sciences, 9,* 585–603.

Bortnik, J., Bleier, T. E., Dunson, C., & Freund, F. T. (2010). Estimating the seismotelluric current required for observable electromagnetic ground signals. *Annals of Geophysics, 28,* 1615–1624.

Buehler, T., Raible, C. C., & Stocker, T. F. (2011). The relationship of winter season North Atlantic blocking frequencies to extreme cold or dry spells in the ERA-40. *Tellus, 63*(2), 212–222.

Cattiaux, J., Vautard, R., Cassou, C., Yiou, P., Masson-Delmotte, V., & Codron, F. (2010). Winter 2010 in Europe: A cold extreme in a warming climate. *Geophysical Research Letters, 37*(20), L20704.

Charney, J. G., & Devore, J. G. (1979). Multiple flow equilibria in the atmosphere and blocking. *Journal of the Atmospheric Sciences, 36,* 1205–1216.

Cicerone, R. D., Ebel, J. E., & Britton, J. (2009). A systematic compilation of earthquake precursors. *Tectonophysics, 476*(3–4), 371–396.

Crepisson, C., Morard, G., Bureau, H., Prouteau, G., Morizet, Y., Petitgirard, S., et al. (2014). Magmas trapped at the continental lithosphere–asthenosphere boundary. *Earth and Planetary Science Letters, 393,* 105–112.

D'Alessandro, F. (2009). Experimental study of the effect of wind on positive and negative corona from a sharp point in a thunderstorm. *Journal of Electrostatics, 67,* 482–487.

D'Andrea, F., Tibaldi, S., Blackburn, M., Boer, G., Déqué, M., Dix, M. R., et al. (1998). Northern Hemisphere atmospheric blocking as simulated by 15 atmospheric general circulation models in the period 1979–1998. *Climate Dynamics, 14,* 385–407.

Da Silva, A. M., & Lindzen, R. S. (1993). On the establishment of stationary waves in the northern-hemisphere winter. *Journal of the Atmospheric Sciences, 50,* 43–61.

de Vries, H., Haarsma, R. J., & Hazeleger, W. (2012). Western European cold spells in current and future climate. *Geophysical Research Letters, 39*(4), L04706.

de Vries, H., Woollings, T., Anstey, J., Haarsma, R. J., & Hazeleger, W. (2013). Atmospheric blocking and its relation to jet changes in a future climate. *Climate Dynamics, 41*(9), 2643–2654.

Dinske, C., & Shapiro, S. A. (2013). Seismotectonic state of reservoirs inferred from magnitude distributions of fluid-induced seismicity. *Journal of Seismology, 17,* 13–25.

Doblas-Reyes, F. J., Casado, M. J., & Pastor, M. A. (2002). Sensitivity of the Northern hemisphere blocking frequency to the detection index. *Journal of Geophysical Research, 107,* 4009.

Dole, R. M., & Gordon, N. D. (1983). Persistent anomalies of the extra-tropical Northern Hemisphere wintertime circulation. Geographical distribution and regional persistence characteristics. *Monthly Weather Review, 111*(8), 1567–1586.

Dubrov, M. N., Volkov, V. A., & Golovachev, S. P. (2014). Earthquake and hurricane coupling is ascertained by ground-based laser interferometer and satellite observing techniques. *Natural Hazards and Earth System Sciences, 2,* 935–961.

Dunajecka, M. A., & Pulinets, S. A. (2005). Atmospheric and thermal anomalies observed around the time of strong earthquakes in México. *Atmósfera, 18*(4), 236–247.

Egger, J. (1978). Dynamics of blocking highs. *Journal of the Atmospheric Sciences, 35,* 1788–1801.

Enescu, B., Mori, J., & Miyazawa, M. (2007). Quantifying early aftershock activity of the 2004 mid-Niigata Prefecture earthquake (Mw 6.6). *Journal of Geophysical Research, 112,* B04310.

Freund, F. T. (2013). Earthquake forewarning—A multidisciplinary challenge from the ground up to space. *Acta Geophysica, 61*(4), 775–807.

Freund, F. T., & Freund, M. M. (2015). Paradox of peroxy defects and positive holes in rocks part I: Effect of temperature. *Journal of Asian Earth Sciences, 2015,* 373–383.

Freund, F. T., Kulahci, I. G., Cyr, G., Ling, J., Winnick, M., Tregloan-Reed, J., et al. (2009). Air ionization at rock surfaces and pre-earthquake signals. *Journal of Atmospheric and Solar-Terrestrial Physics, 71*(17–18), 1824–1834.

Freund, F. T., & Pilorz, S. (2012). Electric currents in the earth crust and the generation of pre-earthquake ULF signals. In M. Hayakawa (Ed.), *Frontier of earthquake prediction studies* (pp. 464–508). Tokyo: Nippon Shuppan.

Grant, R. A., Raulin, J. R., & Freund, F. T. (2015). Changes in animal activity prior to a major (M = 7) earthquake in the Peruvian Andes. *Physics and Chemistry of the Earth A/B/C, 85–86,* 69–77.

Gutenberg, B., & Richter, C. F. (1954). *Seismicity of the earth and its associate phenomena* (2nd ed., p. 310). Princeton: Princeton University Press.

Hansen, A. R., & Sutera, A. (1984). A comparison of the spectral energy and enstrophy budgets of blocking versus non-blocking periods. *Tellus A, 36,* 52–63.

Heraud, J. (2014). Pre-earthquake signals at the ground level. In F. Freund & S. Langhoff (Eds.), *Universe of scales: From nanotechnology to cosmology* (pp. 133–157). Berlin: Springer.

Hijmans, R. J., Cameron, S. E., Parra, J. L., Jones, P. G., & Jarvis, A. (2005). Very high resolution interpolated climate surfaces for global land areas. *International Journal of Climatology, 25*(15), 1965–1978.

Hitchman, M. H., & Huesmann, A. S. (2007). A seasonal climatology of Rossby wave breaking in the 320–2000-K layer. *Journal of the Atmospheric Sciences, 64,* 1922–1940.

Huang, F., Tang, X., Lou, S. Y., & Lu, C. (2007). Evolution of dipole-type blocking life cycles: Analytical diagnoses and observations. *Journal of the Atmospheric Sciences, 64,* 52–73.

Illari, L. (1984). A diagnostic study of the potential vorticity in a warm blocking anticyclone. *Journal of the Atmospheric Sciences, 41,* 3518–3526.

Inan, S., Ertekin, K., Seyis, C., Şimşek, Ş., Kulak, F., Dikbaş, A., et al. (2010). Multi-disciplinary earthquake researches in Western Turkey: Hints to select sites to study geochemical transients associated to seismicity. *Acta Geophysica, 58,* 767–813.

King, B. V., & Freund, F. T. (1984). Surface charges and subsurface space charge distribution in magnesium oxide containing dissolved traces of water. *Physical Review B, 29,* 5814–5824.

Klimenko, M. V., Klimenko, V. V., Zakharenkova, I. E., Pulinets, S. A., Zhao, B., & Tsidilina, M. N. (2011). Formation mechanism of great positive TEC disturbances prior to Wenchuan earthquake on May 12, 2008. *Advances in Space Research, 48,* 488–499.

Kobeissi, M. A., Gomez, F., & Tabet, C. (2015). Measurement of anomalous radon gas emanation across the Yammouneh fault in southern Lebanon: A possible approach to earthquake prediction. *International Journal of Disaster Risk Science, 6,* 250.

Kolarž, P., Gaisberger, M., Madl, P., Hofmann, W., Ritter, M., & Hartl, A. (2012). Characterization of ions at Alpine waterfalls. *Atmospheric Chemistry and Physics, 12,* 3687–3697.

Konrad, C. E., & Colucci, S. J. (1988). Synoptic climatology of 500-mb circulation changes during explosive cyclogenesis. *Monthly Weather Review, 116*(7), 1431–1443.

Lejenäs, H., & Döös, B. (1987). The behaviour of the stationary and travelling planetary-scale waves during blocking—A northern hemispheric data study. *Journal of the Meteorological Society of Japan, 65,* 709–725.

Lejenäs, H., & Økland, H. (1983). Characteristics of Northern Hemisphere blocking as determined from a long time series of observational data. *Tellus, 35A*(5), 350–362.

Lindzen, R. S. (1986). Stationary planetary-waves, blocking, and interannual variability. *Advances in Geophysics, 29,* 251–273.

Liu, J. Y., Chen, Y. I., Huang, C. H., Ho, Y. Y., & Chen, C. H. (2015). A statistical study of lightning activities and M $\geq$ 5.0 earthquakes in Taiwan during 1993–2004. *Surveys in Geophysics, 36*(6), 851–859.

Luo, D. H. (2005). A barotropic envelope Rossby soliton model for block—Eddy interaction. Part IV: Block activity and its linkage with a sheared environment. *Journal of the Atmospheric Sciences, 62,* 3860–3884.

Luo, D. H., Huang, F., & Diao, Y. N. (2001). Interaction between antecedent planetary-scale envelope soliton blocking anticyclone and synoptic-scale eddies: Observations and theory. *Journal of Geophysical Research, 106*(D23), 31795–31815.

Lupo, A. R. (1997). A diagnosis of two blocking events that occurred simultaneously over the midlatitude Northern Hemisphere. *Monthly Weather Review, 125*(8), 1801–1823.

Lupo, A. R., Niemeyer, J., Rabinowitz, J., Hensen, C., Balkissoon, S., Clay, C., Korner, A., Renken, J., Bradshaw, T., & Herman, J. (2014). *Northern hemisphere blocking archive data. Department of soil, environmental and atmospheric sciences*. University of Missouri, Columbia. http://weather.missouri.edu/gcc. Accessed 25 Dec 2014.

Lupo, A. R., & Smith, P. J. (1995). Climatological features of blocking anticyclones in the Northern Hemisphere. *Tellus, 47A*(4), 439–456.

Malguzzi, P., & Malanotte-Rizzoli, P. (1984). Nonlinear stationary Rossby waves on nonuniform zonal winds and atmospheric blocking, part I: The analytical theory. *Journal of the Atmospheric Sciences, 41,* 2620–2628.

Mansouri Daneshvar, M. R. (2015). *Synoptic assessment of the atmospheric precursors in order to foresight of major earthquake events in the Middle East*. PhD Thesis in Climatology and Environmental Planning at Sistan and Baluchestan University **(in Persian)**.

Mansouri Daneshvar, M. R., & Freund, F. T. (2017). Remote sensing of atmospheric and ionospheric signals prior to the Mw 8.3 Illapel earthquake, Chile 2015. *Pure and Applied Geophysics, 174*(1), 11–45.

Mansouri Daneshvar, M. R., Khosravi, M., & Tavousi, T. (2014a). Seismic triggering of atmospheric variables prior to the major earthquakes in the Middle East within a 12-year time-period of 2002–2013. *Natural Hazards, 74*(3), 1539–1553.

Mansouri Daneshvar, M. R., Tavousi, T., & Khosravi, M. (2014b). Synoptic detection of the short-term atmospheric precursors prior to a major earthquake in the Middle East, North Saravan M 7.8 earthquake, SE Iran. *Air Quality, Atmosphere and Health, 7*(1), 29–39.

Mansouri Daneshvar, M. R., Tavousi, T., & Khosravi, M. (2015). Atmospheric blocking anomalies as the synoptic precursors prior to the induced earthquakes; A new climatic conceptual model. *International Journal of Environmental Science and Technology, 12*(5), 1705–1718.

Marshall, A. G., Hudson, D., Hendon, H. H., Pook, M. J., Alves, O., & Wheeler, M. C. (2013). Simulation and prediction of blocking in the Australian region and its influence on intra-seasonal rainfall in POAMA-2. *Climate Dynamics, 42*(11–12), 3271–3288.

McWilliams, J. C. (1980). An application of equivalent modons to atmospheric blocking. *Dynamics of Atmospheres and Oceans, 5*(1), 43–66.

Molchanov, O. (2010). About climate-seismicity coupling from correlation analysis. *Natural Hazards and Earth System Sciences, 10,* 299–304.

Ondoh, T. (2003). Anomalous sporadic-E layers observed before M 7.2 Hyogo-ken Nanbu earthquake; Terrestrial gas emanation model. *Advances in Polar Upper Atmosphere Research, 17,* 96–108.

Ouzounov, D., Liu, D., Chunli, K., Cervone, G., Kafatos, M., & Taylor, P. (2007). Outgoing long wave radiation variability from IR satellite data prior to major earthquakes. *Tectonophysics, 431*(1–4), 211–220.

Ouzounov, D., Pulinets, S., Romanov, A., Romanov, A., Tsybulya, K., Davidenko, D., et al. (2011). Atmosphere-ionosphere response to the M9 Tohoku earthquake revealed by joined

satellite and ground observations: preliminary results. *Earthquake Science, 24,* 557–564.

Pelly, J. L., & Hoskins, B. J. (2003). A new perspective on blocking. *Journal of the Atmospheric Sciences, 60*(5), 743–755.

Pfahl, S., Schwierz, C., Croci-Maspoli, M., Grams, C. M., & Wernli, H. (2015). Importance of latent heat release in ascending airstreams for atmospheric blocking. *Nature Geoscience, 8,* 610–614.

Pulinets, S. A. (2006). Space technologies for short-term earthquake warning. *Advances in Space Research, 37*(4), 643–652.

Pulinets, S. A. (2011). The synergy of earthquake precursors. *Earthquake Science, 24*(6), 535–548.

Pulinets, S. A., Alekseev, V. A., Legen'ka, A. D., & Khegai, V. V. (1997). Radon and metallic aerosols emanation before strong earthquakes and their role in atmosphere and ionosphere modification. *Advances in Space Research, 20*(11), 2173–2176.

Pulinets, S. A., Bondur, V. G., Tsidilina, M. N., & Gapunova, M. V. (2010). Verification of the Concept of Seismoionospheric Coupling under Quiet Heliogeomagnetic Conditions, using the Wenchuan (China) Earthquake of May 12, 2008, as an Example. *Geomagnetism and Aeronomy, 50*(2), 231–242.

Pulinets, S. A., & Dunajecka, M. A. (2007). Specific variations of air temperature and relative humidity around the time of Michoacan earthquake M8.1 Sept. 19, 1985 as a possible indicator of interaction between tectonic plates. *Tectonophysics, 431*(1–4), 221–230.

Pulinets, S. A., & Ouzounov, D. (2010). Lithosphere-atmosphere-ionosphere coupling (LAIC) model—an unified concept for earthquake precursors validation. *Journal of Asian Earth Sciences, 41*(4–5), 371–382.

Pulinets, S. A., & Ouzounov, D. (2011). Lithosphere-atmosphere-ionosphere coupling (LAIC) model—an unified concept for earthquake precursors validation. *Journal of Asian Earth Sciences, 41*(4–5), 371–382.

Pulinets, S. A., Ouzounov, D., Ciraolo, L., Singh, R., Cervone, G., Leyva, A., et al. (2006). Thermal, atmospheric and ionospheric anomalies around the time of the Colima M7.8 earthquake of 21 January 2003. *Annales Geophysicae, 24,* 835–849.

Pulinets, S. A., Ouzounov, D., Karelin, A., & Davidenko, D. (2014). Physical bases of the generation of short-term earthquake precursors: A complex model of ionization-induced geophysical processes in the lithosphere-atmosphere-ionosphere-magnetosphere system. *Geomagnetism and Aeronomy, 55*(4), 522–539.

Rex, D. F. (1950). Blocking action in the middle troposphere and its effects upon regional climate. II. The climatology of blocking action. *Tellus, 2*(4), 275–301.

Richter, C. F. (1958). *Elementary seismology*. San Fransisco: WH Freeman and Co.

Santos, V. N. D., Herrmann, E., Manninen, H. E., Hussein, T., Hakala, J., Nieminen, T., et al. (2015). Variability of air ion concentrations in urban Paris. *Atmospheric Chemistry and Physics, 15,* 13717–13737.

Scaife, A. A., Woollings, T., Knight, J., Martin, G., & Hinton, T. (2010). Atmospheric blocking and mean biases in climate models. *Journal of Climate, 23,* 6143–6152.

Scherrer, S. C., Croci-Maspoli, M., Schwierz, C., & Appenzeller, C. (2006). Two-dimensional indices of atmospheric blocking and their statistical relationship with winter climate patterns in the Euro-Atlantic region. *International Journal of Climatology, 26,* 233–249.

Schwierz, C., Croci-Maspoli, M., & Davies, H. C. (2004). Perspicacious indicators of atmospheric blocking. *Geophysical Research Letters, 31,* L06125.

Scoville, J., Sornette, J., & Freund, F. T. (2015). Paradox of peroxy defects and positive holes in rocks part II: Outflow of electric currents from stressed rocks. *Journal of Asian Earth Science, 114*(Part 2), 338–351.

Shutts, G. J. (1983). The propagation of eddies in diffluent jetstreams—Eddy vorticity forcing of blocking flow-fields. *Quarterly Journal of the Royal Meteorological Society, 109,* 737–761.

Sillmann, J., & Croci-Maspoli, M. (2009). Present and future atmospheric blocking and its impact on European mean and extreme climate. *Geophysical Research Letters, 36*(10), L10702.

Sillmann, J., Croci-Maspoli, M., Kallache, M., & Katz, R. W. (2011). Extreme cold winter temperatures in Europe under the influence of north Atlantic atmospheric blocking. *Journal of Climate, 24*(22), 5899–5913.

Svensmark, H., Pedersen, J. O. P., Marsch, N. D., Enghoff, M. B., & Uggerhøj, U. I. (2007). Experimental evidence for the role of ions in particle nucleation under atmospheric conditions. *Proceedings of the Royal Society A, 463*(2078), 385–396.

Sykes, L. R., Shaw, B. E., & Scholz, C. H. (1999). Rethinking earthquake prediction. *Pure and Applied Geophysics, 155,* 207–232.

Tammet, H., Hõrrak, U., & Kulmala, M. (2009). Negatively charged nanoparticles produced by splashing of water. *Atmospheric Chemistry and Physics, 9,* 357–367.

Thompson, E. M., Baise, L. G., & Vogel, R. M. (2007). A global index earthquake approach to probabilistic assessment of extremes. *Journal of Geophysical Research, 112,* B06314.

Tibaldi, S., & Molteni, F. (1990). On the operational predictability of blocking. *Tellus, 42A*(3), 343–365.

Trigo, R., Trigo, I., Da Camara, C., & Osborn, T. J. (2004). Climate impact of the European winter blocking episodes from the NCEP/NCAR Reanalyses. *Climate Dynamics, 23*(1), 17–28.

Tsou, C. H., & Smith, P. J. (1990). The role of synoptic/planetary scale interactions during the development of a blocking anticyclone. *Tellus, 42A*(1), 174–193.

USGS (2014). *Earthquake archive data*. Online catalog of United States Geological Survey. http://earthquake.usgs.gov/earthquakes. Accessed 20 Oct 2014.

Vautard, R. (1990). Multiple weather regimes over the North Atlantic: Analysis of precursors and successors. *Monthly Weather Review, 118,* 2056–2081.

Verkley, W. T. M. (1990). Modons with uniform absolute vorticity. *Journal of the Atmospheric Sciences, 47*(6), 727–745.

Wiedenmann, J. M., Lupo, A. R., Mokhov, I. I., & Tikhonova, E. A. (2002). The climatology of blocking anticyclones for the northern and southern hemispheres: block intensity as a diagnostic. *Journal of Climate, 15*(23), 3459–3473.

Yada, N., & Saito, Y. (2012). *Precursor observed by movements of aero-ionization measurement prior to the pacific coast of Tohoku earthquake in 2011*. EMSEV 2012. Gotemba, Japan.